JOURNAL OF SOLID STATE CHEMISTRY **17**, 43–48 (1976)

Mössbauer Effect in Single-Crystal $Fe_{1-x}S$

J. R. GOSSELIN, M. G. TOWNSEND, R. J. TREMBLAY, AND A. H. WEBSTER

Mineral Sciences Laboratories, Canada Centre for Mineral and Energy Technology, Department of Energy, Mines and Resources, Ottawa, Canada K1A OG1

Received May 5, 1975; in revised form August 7, 1975.

Mössbauer spectra have been recorded for single crystals of very nearly stoichiometric FeS and $Fe_{0.93}S$ at temperatures between 80 and 600°K. The spectra of nearly stoichiometric FeS indicate that the low-temperature 2C structure with spins $\parallel c$ preserves the spin orientation $\parallel c$ during the structural transformation to $1C$ at T_α ($\doteq 420$°K). However, because of a miscibility gap, a few percent of the high-temperature $1C$ structure with spins $\perp c$ is present even at 300°K and the concentration of this component increases with temperature. At T_s ($\doteq 445$°K) the spins in the $1C$ structure that are $\parallel c$ rotate to $\perp c$. In $Fe_{0.93}S$, the hyperfine splittings indicate that the rotation of the spins from $\parallel c$ to $\perp c$ at 170°K is a first-order process.

1. Introduction

The separate identity of the structural transition at T_α and the magnetic transition at T_s in FeS was established by neutron diffraction in carefully annealed powder specimens of nearly stoichiometric material (*1*, *2*). These measurements, however, were not able to identify the precise composition of the magnetic phases at temperatures close to T_α and T_s.

The Mössbauer spectra of polycrystalline $Fe_{1-x}S$ have been studied extensively (*3*). Some Mössbauer studies have also been reported on a single-crystal of $Fe_{1-x}S$ of composition somewhat removed from stoichiometric (*4*). In contrast to these Mössbauer studies, the material used in the present work (a well-annealed single crystal of very nearly stoichiometric FeS) was sufficiently homogeneous to allow the transitions at T_α and T_s to be sharp and clearly separated, as indicated by magnetic susceptibility (*5*). This allows unambiguous identification of the nature of the magnetic phases at temperatures close to T_α and T_s.

Powder neutron diffraction in nonstoichiometric $Fe_{1-x}S$ indicated the presence of transitions below room temperature (*1*); such transitions had not been examined by Mössbauer spectroscopy prior to the present work.

2. Experimental Procedure

Single crystals of $Fe_{0.996}S$ and $Fe_{0.93}S$ were grown by the Bridgman method in sealed evacuated silica capsules. The $Fe_{0.996}S$ and the $Fe_{0.93}S$ crystals were annealed at 850°C for 10 days and at 600°C for 8 days, respectively. The details of their preparation and characterization are given in (*5*). For determination of Mössbauer spectra, plates were cut from the same boules that were used in magnetic susceptibility, DTA, and thermoelectric power measurements (*5*). The plates were cemented to glass slides 0.003 in. thick and were thinned to from 0.002 to 0.001 in. thick. Mössbauer spectra were obtained at temperatures between 78 and 600°K using a spectrometer with a source of ^{57}Co in a Cu matrix and with constant acceleration drive. Temperatures were controlled to within less than ±0.5°K. The spectra were computer fitted to a given number of Lorenzian lineshapes with correction for a parabolic background by a least-squares iterative procedure. Line positions and half-widths were allowed to float freely except in the case of a few lines,

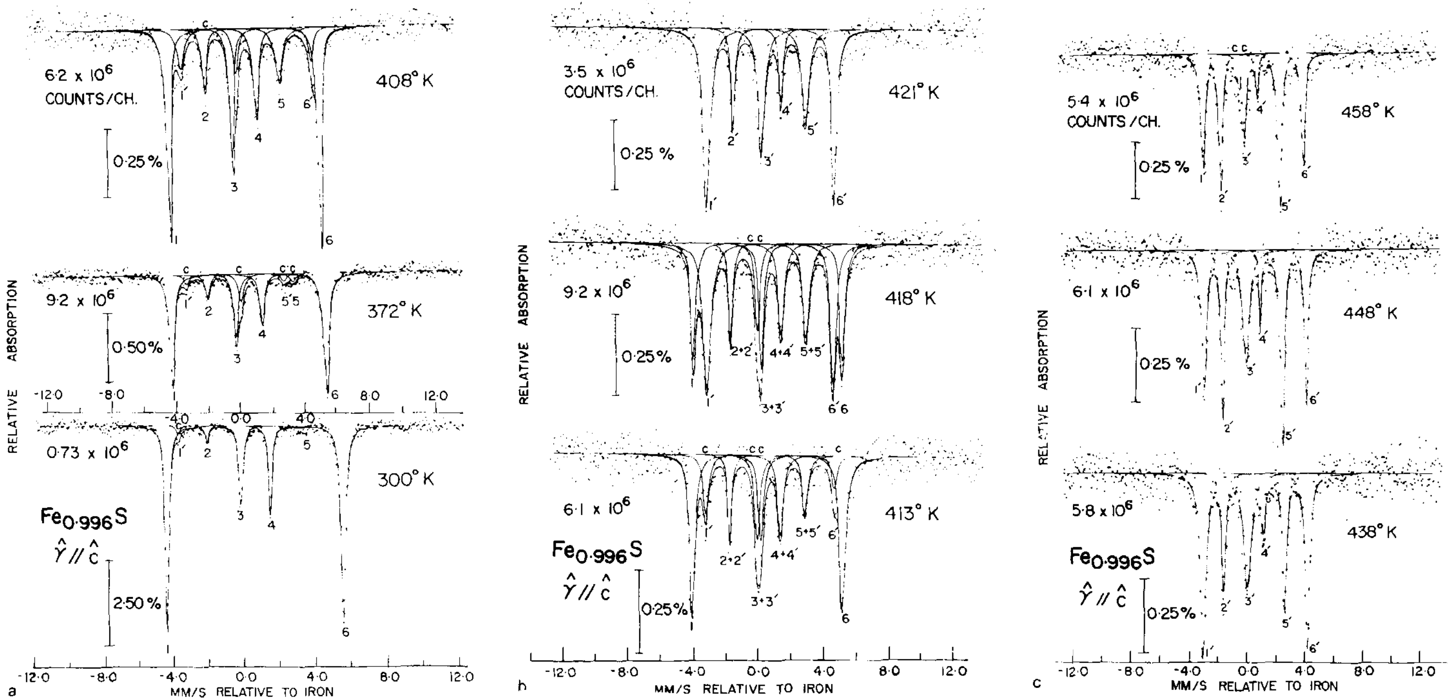

FIG. 1. Mössbauer spectra of single crystal $Fe_{0.996}S$, for γ-ray ∥c direction. Line positions and widths were allowed to float freely in the computer fit, except for lines marked *c*, where the half-widths were constrained. Extra intensity at line 3 in some spectra is due to stainless steel.

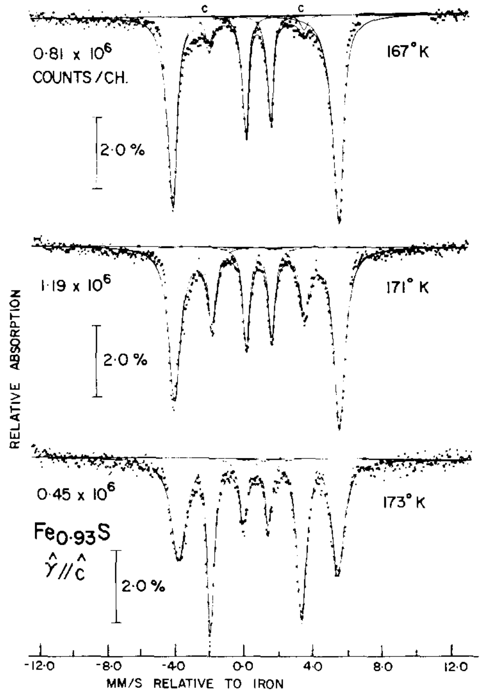

FIG. 2. Mössbauer spectra of single-crystal $Fe_{0.93}S$ for γ-ray $\parallel c$ direction. Line positions and widths were allowed to float freely in the computer fit, except for lines marked c where the half-widths were constrained.

marked by c in Figs. 1a–c and Fig. 2, where the half-widths only were constrained. The velocity scale was calibrated before or after every spectrum using metallic iron powder as standard. The average width at half-height of the lines in the iron spectrum is 0.33 mm/sec, approximately the same as in the spectrum of $Fe_{0.996}$.

3. Results and Discussion

3.1. *Mössbauer Spectra in* $Fe_{0.996}S$

To first order, the relative intensities of a Mössbauer magnetic hyperfine spectrum are (3:0:1) for spins $\parallel$ the γ-ray direction and (3:4:1) for spins $\perp$ the γ-ray direction.

The Mössbauer spectrum at 300°K of $Fe_{0.996}S$ oriented with the c-axis $\parallel$ the γ-ray direction (Fig. 1a) shows weak lines (2, 5, and 1′) in addition to the four strong lines (1, 3, 4 and 6) anticipated for spins $\parallel$ the γ-ray direction and $\parallel c$ in the 2C structure. Lines 2 and 5 result both from a slight misorientation of the crystal and the fact that the γ-rays are not perfectly collimated, whereas line 1′ arises from the high-temperature hexagonal 1C phase. With increasing temperature the relative intensity of this line increases and simultaneously line 6′ resolves from line 6. Figure 1b (418°K) shows that the concentration of the high-temperature phase, as indicated by the relative growth of the primed peaks, increases dramatically at T_α and that at 421°K all of the 2C structure appears to have transformed to this phase.

The relative intensity of peaks 1′ and 6′ to 2′ and 5′ in the spectrum taken at 408°K (Fig. 1a) indicates that the spins are $\perp c$ in the high-temperature 1C phase. This is compatible with the phase diagram (see Fig. 1 in *5*) on two counts; first, the miscibility gap allows for the crystallographic coexistence of these two phases (1C and 2C) of distinct compositions, and second, the x-dependence of the boundary $T_\alpha(x)$ accounts for the growth of the 1C component with increasing temperature from its traces (peak 1′) at 300°K.

Furthermore, for a small temperature interval, between about 413°K and 421°K (T_α), there is coexistence of the three magnetic phases (2C with spins $\parallel c$, 1C with spins $\parallel c$, and 1C with spins $\perp c$), again in agreement with the phase diagram.

Once above T_α however, the changeover from 1C–$\parallel c$ to 1C–$\perp c$ does not occur abruptly at the $T_s(x)$ corresponding to the nominal composition, but is rather gradual as witnessed by the relative intensities of peaks 1′ and 6′ to peaks 2′ and 5′ in Fig. 1b and c; this progressive transition results from a small spread in composition around the nominal one since, as pointed out in the magnetic anisotropy data (*5*), the spins do not rotate gradually over a temperature interval but flip locally [at $T_s(x)$] by 90°.

The foregoing results are summarized in Fig. 3, where the relative spin concentrations estimated from the area under their respective spectra are plotted as a function of temperature. Andresen and Torbo (*1*) monitored the powder intensities of the (21$\bar{3}$1) neutron lattice superreflection and the neutron magnetic (0001) reflection. However, from their

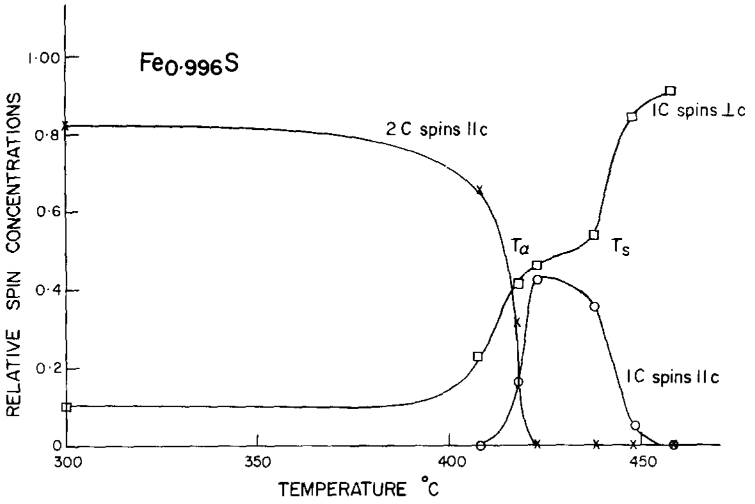

FIG. 3. Relative spin concentrations in $Fe_{0.996}S$, as a function of temperature.

results, they were not able to identify the growth of the $1C$ component with spins $\parallel c$ at T_α (Fig. 3).

The above structural and magnetic transformations, while readily traceable via the relative peak positions and intensities, also can be followed through the changes in the respective quadrupolar shifts. In Fig. 4 are shown the shifts defined by (a) $\frac{1}{4}[(V_3 - V_1) - (V_6 - V_4)]$ for the $2C$ structure, and (b) $\frac{1}{4}[(V_2' - V_1') - (V_6' - V_5')]$, and (c) $\frac{1}{4}[(V_3' - V_1') - (V_6' - V_4')]$ for the $1C$ structure, where V is the velocity in millimeters per second of the respective line.

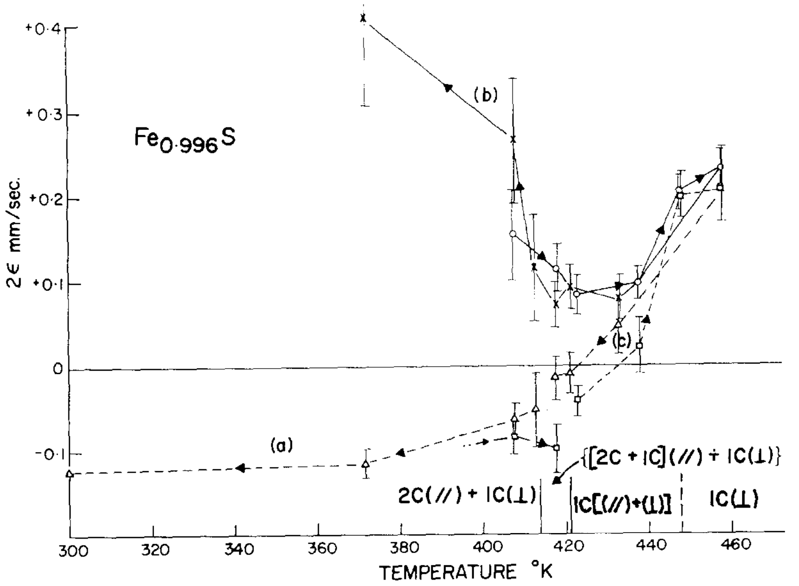

FIG. 4. Quadrupole shifts in $Fe_{0.996}S$; (a) 2ε in $2C$ structure, (b) and (c) 2ε in high-temperature phase, as defined in text.

Below T_α, in the $2C$ structure, the quadrupole shift (a), Fig. 4, is negative and approximately constant with temperature; here the spins are $\parallel c$. At T_α, the absolute magnitude of the shift decreases slightly as the $2C$ structure transforms to the high-temperature $1C$ phase with spins $\parallel c$.

At temperatures between 300 and 400°K, the spins are $\perp c$ in the minor high-temperature $1C$ phase, and the quadrupole shift (*b*) is positive (Fig. 4). At T_α, the $2C$ structure transforms to high-temperature $1C$ phase with spins $\parallel c$, with a negative quadrupole shift; the two spin components in the high-temperature $1C$ phase now coexist above T_α, but the individual lines of each hyperfine component are too broad to be separately resolved. There is therefore an apparent decrease in the value of (b) at T_α ($\simeq 420$°K); see Fig. 4. Because of this coexistence above T_α of spins $\parallel c$ and $\perp c$ in the high-temperature $1C$ phase, and the fact that the position of lines 2′ and 5′ depend only on the component with spin $\perp c$ (whereas the position of lines 1′, 3′, 4′ and 6′ depend on both spin components), curve (*b*) does not coincide with curve (c) in this temperature range. At T_s, the value of (b) increases as those spins that are $\parallel c$ in the high-temperature $1C$ phase rotate to $\perp c$. Finally, above T_s, when all the spins are $\perp c$, curve (b) is approximately coincident with curve (c).

The coexistence of two phases below T_α was noted previously by Thiel from Mössbauer measurements on polycrystalline FeS (*3*). A coexistence of two phases has also been observed, by Mössbauer spectroscopy, at the first order phase transition in NiS doped with Fe^{57} (*6*).

Also available from Mössbauer spectra, the magnetic hyperfine splitting drops sharply at T_α from about 290 kOe below T_α to 250 kOe above T_α. The decrease is due at least in part to a decrease in the Fermi-contact term corresponding to the fall in exchange energy at T_α noted earlier with the magnetic susceptibility (*5*). The change in the dipolar contribution to the hyperfine field is likely to be small as the spins remain $\parallel c$ through the transition. There appears to be no significant change in hyperfine splitting at T_s.

The isomer shifts of Fe$_{0.996}$S, Fe$_{0.93}$S, and Fe$_7$S$_8$ are shown in Table I. Hazony (*7*) has related the I.S., quadrupole splitting, and magnetic hyperfine splitting, of a series of Fe^{2+} compounds including FeS by allowing for differential expansion of $\langle r^{-3}\rangle$ for t_{2g} and e_g $3d$ wavefunctions with increasing covalency. In this approach, Fe in FeS is considered to be divalent and relatively covalent. While this works well for quadrupole splitting and isomer shift, in order to be consistent he requires a positive sign of magnetic field at the Fe nucleus in FeS. However, the sign of the magnetic field in ferrimagnetic Fe$_7$S$_8$ is negative as in Fe metal (*8*), and the similarity of the chemical bonding in FeS and Fe$_7$S$_8$ shown by the proximity of the isomer shifts Table I, means that almost certainly the sign of the internal field in FeS is in fact also negative. The absolute magnitude of the hyperfine field (~300 kOe) does not vary greatly in the range FeS to Fe$_7$S$_8$, and it is unlikely that any of the three contributions to the hyperfine field, Fermi contact, dipolar, and orbital fields could vary sufficiently in this range to produce a difference in sign in their algebraic sum.

TABLE I

ISOMER SHIFT AT 300°K VERSUS COMPOSITION

	I.S.mm/sec (with respect to iron) at 300°K
Fe$_{0.996}$S	0.74
Fe$_{0.93}$S	0.69
Fe$_7$ S$_8$	0.66[a]

[a] Ref. (*8*).

The above suggests that other factors need to be considered in the phenomenological approach proposed by Hazony.

The isomer shift of Fe$_{0.996}$S decreases slowly with increasing temperature and reaches about 0.62 mm/sec at 400°K. There is no abrupt decrease in I.S. at T_α, in agreement with (*3*), giving no evidence for a sudden delocalisation of the *d* electrons at T_α. We also deduce that the contribution of covalency to the change in hyperfine field at T_α is negligible.

Unrelated to the above description is the anomalous intensity of peak 3 in Fig. 1: this

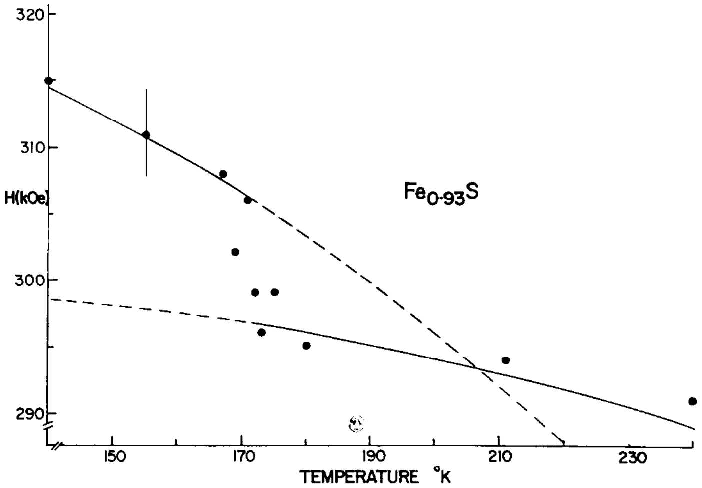

FIG. 5. Mössbauer hyperfine field versus temperature for $Fe_{0.93}S$.

results from absorption by stainless steel in the faces of the temperature cell. It does not occur in the spectrum at 300°K where the sample was not in the cell, nor is it apparent in the spectra of $Fe_{0.93}S$ where the number of counts is lower (Fig. 2). This absorption is taken into account in the analysis.

3.2. Mössbauer Spectra in $Fe_{0.93}S$

Some of the Mössbauer spectra recorded on single crystals of $Fe_{0.93}S$ oriented with the c-axis $\parallel$ the γ-ray direction are shown in Fig. 2. The rotation of the spins from $\parallel c$ to $\perp c$ at $T \sim 170°K$ is quite apparent. In the transition region, which is no more than 6°K wide (Fig. 5), the relative intensities of the hyperfine pattern indicate a coexistence of the two spin configurations. The magnetic hyperfine splitting drops sharply at T_s (Fig. 5), indicating a first-order transition. The quadrupole shift defined by $2\varepsilon = \frac{1}{4}\{(V_3 - V_1) - (V_6 - V_4)\}$ changes sign at T_s as the spins rotate.

It is not known if the iron vacancies in $Fe_{0.93}S$ are ordered at T_s as there have been no X-ray measurements in this temperature range. However, at room temperature our X-ray measurements indicate the presence of a $5C$ hexagonal superlattice. The Mössbauer lines are broad, the average width at half-height is 0.55 mm/sec, and it is not possible to discern a regular splitting pattern such as is the case in Fe_7S_8 where the vacancies are ordered in a $4C$ superlattice (*8*). This may be due to the fact that the many different sites in the $5C$ superlattice have parameters too close to allow resolution; a model for $5C$ $Fe_{0.93}S$ has been proposed by Schwarz and Vaughan (*9*).

Acknowledgments

The authors thank J. F. Rowland for single-crystal X-ray measurements, D. W. Carson for assistance with computer fitting of Mössbauer spectra, and J. H. G. Laflamme for thinning the crystals for Mössbauer measurements.

References

1. A. F. ANDRESEN AND P. TORBO, *Acta. Chem. Scand.* **21**, 2841 (1967).
2. J. T. SPARKS, W. MEAD AND T. KOMOTO, *J. Phys. Soc. Japan* **17**, Suppl. B-1, 249 (1962).
3. R. C. Thiel, Doctoral thesis, University of Groningen (1969).
4. H. HORITA AND E. HIRAHARA, *Science Repts. (Tohoku Univ.)* **54**, 127 (1971).
5. J. L. HORWOOD, M. G. TOWNSEND, AND A. H. WEBSTER, *J. Solid State Chem.* **17**, (1976).
6. J. R. GOSSELIN, M. G. TOWNSEND, R. J. TREMBLAY, L G. RIPLEY, AND D. W. CARSON, *J. Phys. C.: Solid State Phys.* **6**, 1661 (1973).
7. Y. HAZONY, *Phys. Rev.* **B3** (1971).
8. J. R. GOSSELIN, M. G. TOWNSEND, R. J. TREMBLAY, AND A. H. WEBSTER, *Mater. Res. Bull.* **10**, 41 (1975).
9. E. J. SCHWARZ AND D. J. VAUGHAN, *J. Geomag. Geoelect.* **24**, 441 (1972).